ACS ORGANIC & INORGANIC Au
AN OPEN ACCESS JOURNAL OF THE AMERICAN CHEMICAL SOCIETY

pubs.acs.org/orginorgau

Article

Expeditive Synthesis of Potent C20-*epi*-Amino Derivatives of Salinomycin against Cancer Stem-Like Cells

Dominika Czerwonka, Sebastian Müller, Tatiana Cañeque, Ludovic Colombeau, Adam Huczyński, Michał Antoszczak,* and Raphaël Rodriguez*

Cite This: *ACS Org. Inorg. Au* 2022, 2, 214–221

Read Online

ACCESS | Metrics & More | Article Recommendations | Supporting Information

ABSTRACT: As a continuation of our studies toward the development of small molecules to selectively target cancer stem cells (CSCs), a library of 18 novel derivatives of salinomycin (**Sal**), a naturally occurring polyether ionophore, was synthesized with a good overall yield using a one-pot Mitsunobu–Staudinger procedure. Compared to the parent structure, the newly synthesized products contained the mono- or disubstituted C20-*epi*-amine groups. The biological activity of these compounds was evaluated against human mammary mesenchymal HMLER CD24^{low}/CD44^{high} cells, a well-established model of breast CSCs, and its isogenic epithelial cell line (HMLER CD24^{high}/CD44^{low}) lacking CSC properties. Importantly, the vast majority of **Sal** derivatives were characterized by low nanomolar activities, comparing favorably with previous data in the literature. Furthermore, some of these derivatives exhibited a higher selectivity for the mesenchymal state compared to the reference **Sal** and ironomycin, representing a promising new series of compounds with anti-CSC activity.

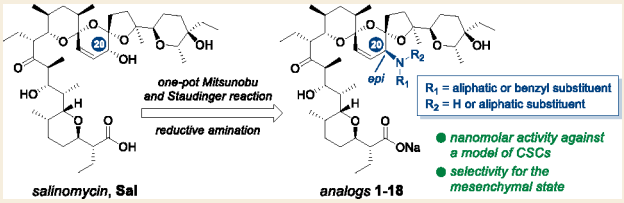

KEYWORDS: *salinomycin, Mitsunobu reaction, Staudinger reaction, cancer stem cells, anticancer activity*

1. INTRODUCTION

There is an urgent need to develop new cancer therapeutics.[1] Particularly interesting in this context are molecules that could preferentially target a fraction of cancer cells, known as cancer stem cells (CSCs).[2,3] These cells can be refractory to conventional chemotherapy and radiation therapy, leading to disease recurrence and metastasis.[4,5]

Using a high-throughput screening method, Gupta et al. identified the natural product salinomycin (**Sal**) as a selective inhibitor of breast CSCs among ∼16 000 compounds tested.[6] Since **Sal** was reported to be active against CSCs of various tissue types,[7,8] intensive studies have been performed to elucidate the mechanism of action (MoA) of **Sal**. In addition to other effects, **Sal** has been shown to alter mitochondrial functions, decrease ATP levels, and alter autophagy.[9−11] Moreover, **Sal** has also been evidenced to induce stress in the endoplasmic reticulum (ER) by altering Ca^{2+} homeostasis.[12]

Regarding its promising anticancer potential, many research groups have attempted to develop more effective chemical modifications of **Sal**,[13] particularly through the derivatization of the C1-carboxyl[14−19] or C20-hydroxyl.[20−24] Using a series of chemo- and stereocontrolled reactions, we successfully modified the C20-hydroxyl of **Sal** to obtain a series of potent C20-amino analogs.[20,21] The highly promising molecule in this group, ironomycin (Figure 1), had been found to be approximately 10-fold more active against breast CSCs than the unmodified **Sal** both *in vitro* and *in vivo*.[21]

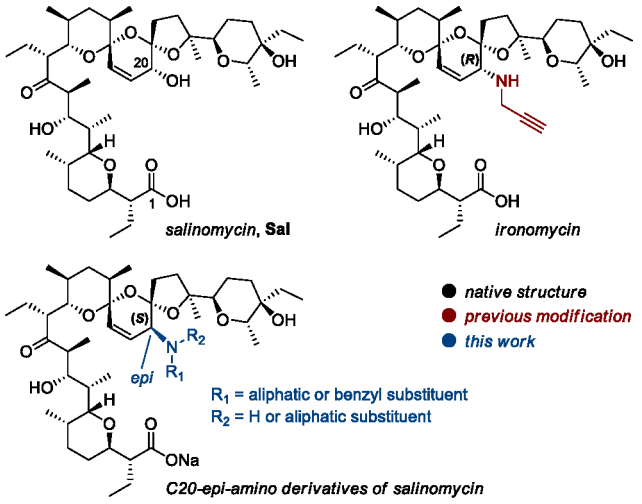

Figure 1. Molecular structures of the parent natural product salinomycin, a potent C20-amino derivative previously reported by us, and a novel series with C20-*epi*-amino substituents.

Received: November 3, 2021
Revised: December 18, 2021
Accepted: December 21, 2021
Published: January 5, 2022

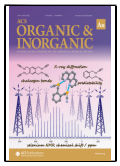

ACS Publications

© 2022 The Authors. Published by American Chemical Society

https://doi.org/10.1021/acsorginorgau.1c00046
ACS Org. Inorg. Au 2022, 2, 214–221

Scheme 1. Synthesis of C20-*epi*-Amino Derivatives of Salinomycin[a]

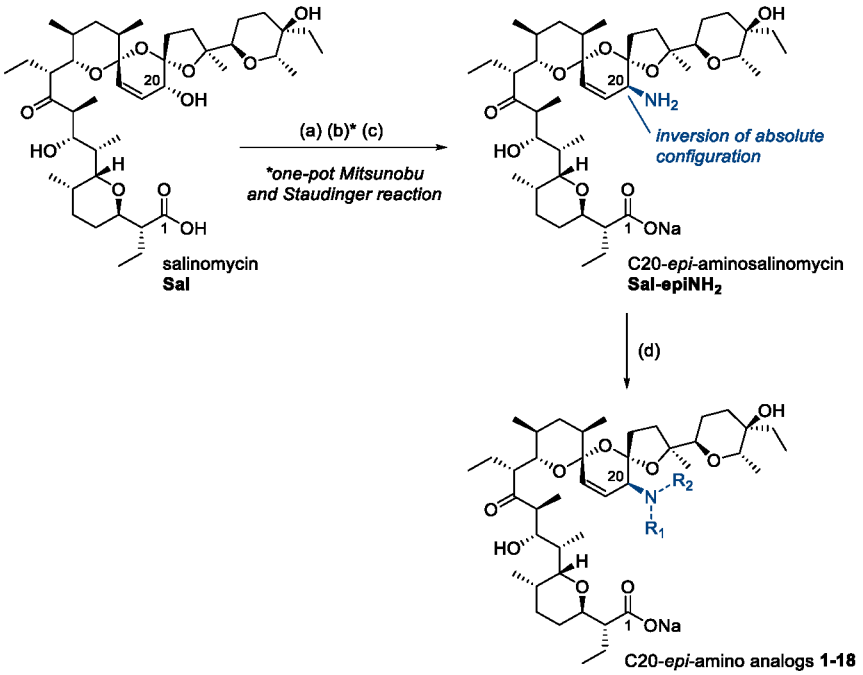

Comp.	R_1 =	R_2 =
1 (70%)	$-CH_2CH_3$	-H
2 (66%)	$-(CH_2)_2CH_3$	-H
3 (68%)	$-(CH_2)_3CH_3$	-H
4 (74%)	$-CH_2CH(CH_3)_2$	-H
5 (82%)	$-(CH_2)_4CH_3$	-H
6 (70%)	$-(CH_2)_5CH_3$	-H
7 (85%)	$-(CH_2)_{11}CH_3$	-H
8 (76%)	$-CH_2CH_3$	$-CH_2CH_3$
9 (79%)	$-(CH_2)_2CH_3$	$-(CH_2)_2CH_3$
10 (55%)	$-(CH_2)_3CH_3$	$-(CH_2)_3CH_3$
11 (60%)	$-(CH_2)_4CH_3$	$-(CH_2)_4CH_3$
12 (82%)	$-(CH_2)_5CH_3$	$-(CH_2)_5CH_3$
13 (45%)	$-(CH_2)_{11}CH_3$	$-(CH_2)_{11}CH_3$
14 (75%)	$-CH_2$-Ph	-H
15 (76%)	$-CH_2$-Ph-OH	-H
16 (89%)	$-CH_2$-Ph-CH_3	-H
17 (88%)	$-CH_2$-Ph-F	-H
18 (58%)	$-CH_2$-Ph-Cl	-H

[a]Reagents and conditions are as follows: (a) DMAP, TMSEtOH, TCFH, CH_2Cl_2, 0 °C to RT; (b) TPP, DIAD, DPPA, THF, RT, then TPP, H_2O, THF, RT; (c) TBAF, THF, RT, then aq. Na_2CO_3; (d) RCHO, CH_2Cl_2, RT, then $NaBH_3CN$, MeOH, RT.

Table 1. Antiproliferative Activity (IC_{50}, μM) with Standard Deviation and Selectivity Index (SI) Values of the C20-*epi*-Amino Derivatives of Salinomycin Measured at 72 h in HMLER $CD24^{low}/CD44^{high}$, HMLER $CD24^{high}/CD44^{low}$, and MCF10A Cells[a]

	HMLER $CD24^{low}/CD44^{high}$	HMLER $CD24^{high}/CD44^{low}$	SI (HMLER)	MCF10A
Sal	1.39 ± 0.10	4.36 ± 0.50	3.1	1.13 ± 0.14
Sal-epiNH$_2$	20.48 ± 3.30	>50	n.d.	>12.5
ironomycin	0.17 ± 0.02	2.28 ± 0.16	13.4	0.12 ± 0.02
1	0.53 ± 0.08	3.25 ± 3.30	6.1	2.61 ± 0.78
2	0.17 ± 0.02	1.71 ± 0.40	10.1	1.56 ± 0.68
3	0.12 ± 0.02	1.83 ± 0.70	15.2	1.46 ± 0.08
4	0.07 ± 0.05	0.77 ± 0.46	11.0	1.30 ± 0.46
5	0.11 ± 0.03	1.19 ± 0.60	10.8	0.46 ± 0.27
6	0.03 ± 0.01	0.74 ± 0.29	24.7	1.50 ± 0.50
7	0.17 ± 0.04	0.69 ± 0.05	4.1	n.d.
8	0.003 ± 0.0005	0.27 ± 0.04	90.0	1.39 ± 0.18
9	0.009 ± 0.0002	0.18 ± 0.02	20.0	0.47 ± 0.19
10	0.85 ± 0.22	6.48 ± 0.50	7.6	n.d.
11	0.33 ± 0.12	2.53 ± 1.00	7.7	3.93 ± 0.29
12	0.30 ± 0.16	3.98 ± 2.20	13.3	1.70 ± 0.44
13	1.92 ± 0.50	10.02 ± 3.60	5.2	n.d.
14	0.12 ± 0.003	0.75 ± 0.12	6.2	4.67 ± 0.73
15	0.10 ± 0.01	1.24 ± 0.02	12.4	4.16 ± 0.57
16	0.07 ± 0.04	0.89 ± 0.28	12.7	1.26 ± 0.18
17	0.06 ± 0.01	0.61 ± 0.01	10.2	1.88 ± 0.11
18	0.08 ± 0.02	0.88 ± 0.54	11.0	1.86 ± 0.31

[a]The selectivity index (SI) was defined as IC_{50}(HMLER $CD24^{high}/CD44^{low}$)/IC_{50}(HMLER $CD24^{low}/CD44^{high}$). Each IC_{50} value was determined in biological triplicate (three independent biological experiments), and each triplicate was determined in at least technical duplicate; n.d., not determined.

Mechanistically, we have provided robust evidence that **Sal**, ironomycin, and other analogs exert their activity by accumulating in lysosomes and sequestering iron in this organelle, which can lead to the production of reactive oxygen species (ROS), lipid peroxidation, and cell death reminiscent of ferroptosis.[21] As cells in the mesenchymal state and CSCs are addicted to iron showing a higher load,[25] this cell state has a pronounced vulnerability to cell death induced by ironomycin and **Sal**.

Given that **Sal** and ironomycin have been found to target lysosomal iron, we hypothesized that a distinct orientation of the C20-amino substituents might affect its stability and target

https://doi.org/10.1021/acsorginorgau.1c00046
ACS Org. Inorg. Au 2022, 2, 214−221

engagement as well as efficacy and selectivity toward the CSC populations. In this context, the synthetic strategy for the diastereoselective inversion of the absolute configuration at the C20-position of **Sal** has been reported previously.[26−29] The esters of C20-*epi*-salinomycin showed a potent activity toward colorectal, gastric, and triple-negative breast cancer cells,[28] while the corresponding C20-*epi*-carbonates and carbamates were identified as inducers of late apoptosis in colon cancer and necrosis in prostate cancer cells.[29] Jiang and co-workers synthesized a series of C20-*epi*-*N*-acyl[26] and C20-*epi*-triazole[27] analogs of **Sal**, showing improved properties compared to **Sal**.

Thus, we were interested in evaluating the effect of combining the presence of an amine at C20 together with the opposite stereochemistry. Here, we describe rapid access to the C20-*epi*-amino derivatives of **Sal** (Figure 1 and Scheme 1). We evaluated a library of 18 novel **Sal** derivatives against a well-established model of breast CSCs together with the corresponding cells deprived of stem-like properties (Table 1). We identified three compounds that have the ability to preferentially kill the cancer stem-like cells with remarkably low IC_{50} values that compete favorably with our reference compound ironomycin. All products were also less toxic against the normal breast cell line MCF10A compared to ironomycin, illustrating some degree of improvement (Table 1).

2. RESULTS AND DISCUSSION

2.1. Synthesis

Although the synthetic access to our key precursor, C20-*epi*-aminosalinomycin **Sal-epiNH$_2$**, has been previously reported,[26] we were able to improve on this procedure. It was conveniently afforded using a one-pot Mitsunobu and Staudinger methodology (Scheme 1), which is important when it comes to scaling up biologically active compounds for therapeutic use. Briefly, in the first step we masked the C1-functionality of **Sal** by converting the C1-carboxyl to a TMS ethyl ester. Next, using a Mitsunobu−Staudinger reaction sequence, followed by quantitative deprotection of the C1-position with TBAF, we obtained **Sal-epiNH$_2$** on a gram scale.

Having facile access to the starting material, a library of 18 C20-*epi*-amino derivatives of **Sal** was synthesized with a good overall yield by means of a chemoselective reductive amination, reacting **Sal-epiNH$_2$** with structurally diverse aldehydes (Scheme 1). Specifically, we used aldehydes that differed in polarity and flexibility, selecting both aliphatic and aromatic substrates. We selected aldehydes with shorter or longer aliphatic chains, from 2 to up to 12 carbon atoms, and various benzyl aldehydes substituted at the *para*-position with a methyl group, a hydroxyl group, or halogens. Importantly, we were able to obtain the corresponding secondary and tertiary amines at the C20-position by varying the amount of aldehyde employed in the reaction mixture. The NMR data of analogs **1**−**18** obtained as sodium salts are presented in the Supporting Information. The HRMS analysis (Supporting Information) also supported the formation of the products.

2.2. Biological Evaluation

The activity of our benchmark compounds **Sal** and ironomycin, together with those of **Sal-epiNH$_2$** and the new derivatives **1**−**18**, was measured *in vitro* against transformed human mammary mesenchymal HMLER CD24^{low}/CD44^{high} cells, an established model of human breast CSCs.[30,31] We also evaluated these products for their selectivity toward the corresponding epithelial counterparts (HMLER CD24^{high}/CD44^{low}), which lacked features of CSCs (Table 1).

Notably, C20-*epi*-amino derivatives exhibited higher anti-CSC potentials compared to **Sal**. Of note, most of these products also showed an improved potency compared to that of the reference ironomycin, among which compounds **4**, **6**, **8**, **9**, and **16**−**18** were the most potent of this series. A deeper analysis of the results revealed that tertiary amine-containing **Sal** derivatives were essentially less potent than their corresponding secondary amine counterparts, with the exceptions of **8** and **9** bearing diethyl and dipropyl substituents, respectively. These derivatives were the most potent compounds, with remarkably low IC_{50} values of 3 and 9 nM against mesenchymal HMLER CD24^{low}/CD44^{high} cells, respectively. Remarkably, the antiproliferative activity of **8** and **9** was accompanied by their higher selectivity for the mesenchymal state, with SIs of 90.0 and 20.0, respectively. This is consistent with iron-targeting and the higher iron demand of that cell state. These data indicate the promising therapeutic potential for **8** and **9** in light of preclinical results already obtained for the less potent lead structure ironomycin. With respect to the other tertiary amines, further elongation of the aliphatic chains resulted in reduced antiproliferative activity, with the didodecyl derivative **13** identified as the least potent of the series. This argues in favor of a model whereby an optimal apolar alkane is required for this biological activity. Analogs with alkanes that are too long might be retained in lipid membranes, up to a point where their capacity to accumulate in the lumen of lysosomes and thus engage with iron is reduced. On the other hand, a critically short side chain may not allow the derivative to effectively cross lipid membranes.

Interestingly, this class of compounds showed generally lower toxicities against the normal breast cell line MCF10A (Table 1), highlighting the potential for the development of these compounds to target CSCs selectively. All analogs were less active against the MCF10A cell line than reference ironomycin, indicating that an inversion of the absolute configuration at the C20-position may improve not only the antiproliferative activity against cancer cells but also the selectivity.

Although monosubstituted C20-*epi*-amino analogs **1** and **2** were found to be less effective than their corresponding disubstituted counterparts **8** and **9**, compound **6** bearing an *n*-hexyl aliphatic chain showed potent antiproliferative activity and selectivity for the mesenchymal state of cells. With an IC_{50} value of 30 nM toward HMLER CD24^{low}/CD44^{high} cells and a good selectivity (SI = 24.7), this compound was the most potent among all secondary amine products. It exhibited a potency comparable to those of **8** and **9**, supporting the importance of an optimal overall lipophilicity, which remains comparable for these three derivatives. It is consistent with the capacity of these derivatives to effectively cross lipid membranes to reach their functional target. Finally, C20-*epi*-amino derivatives **14**−**18** with a benzyl moiety exhibited comparable activities against HMLER CD24^{low}/CD44^{high} cells, with IC_{50} values in the range of 60−120 nM. Interestingly, in all cases the introduction of the substituents (methyl, hydroxyl, or halogen) at the *para*-position resulted in increased selectivity. Thus, the evaluation of the activity of other monosubstituted products (*para*-position versus *ortho*- and *meta*-positions) or multiple-substituted analogs might be worth considering in the future.

3. CONCLUSIONS

In summary, prompted by the improved therapeutic potential of C20-amino analogs of **Sal** (*e.g.*, ironomycin) and the fact that

https://doi.org/10.1021/acsorginorgau.1c00046
ACS Org. Inorg. Au 2022, 2, 214−221

C20-functionalized epimers retain their efficacy *in vitro*, we synthesized a series of 18 C20-*epi*-amino derivatives of **Sal** that combined both structural modifications using a straightforward and scalable protocol.

All derivatives were assessed for their antiproliferative activity and selectivity toward a well-established model of mesenchymal CSCs (HMLER $CD24^{low}/CD44^{high}$) together with their epithelial counterparts (HMLER $CD24^{high}/CD44^{low}$) lacking CSC properties. Most of these derivatives were found to be more potent and more selective against the mesenchymal state compared to the references **Sal** and ironomycin. Specifically, compounds **6**, **8**, and **9** were identified to be particularly interesting in this context, with IC_{50} values of 30, 3, and 9 nM, respectively, together with their outstanding selectivities (SIs between 20.0 and 90.0). Concerning a structure−activity relationship (SAR), we found the following: (i) monosubstituted C20-*epi*-amino derivatives of **Sal** are essentially more active than their corresponding disubstituted counterparts; (ii) with respect to secondary amine products, *n*-pentyl and *n*-hexyl substituents are more potent against the mesenchymal state, (iii) regarding tertiary amine derivatives, elongation of the aliphatic chains results in a decrease of the antiproliferative activity; and (iv) the introduction of the nonpolar or polar substituent at the *para*-position of the benzyl motif increases the selectivity.

Here, we have reported a convenient synthetic scheme that can readily afford potent derivatives in a short number of steps. Importantly, we describe the most potent and selective derivatives of **Sal** reported so far. Future work will involve the preclinical evaluation of the most promising compounds in various cancer settings.

4. EXPERIMENTAL SECTION

4.1. General Information

Detailed descriptions of the general procedures, equipment, and measurement parameters can be found in the Supporting Information. C20-*epi*-aminosalinomycin (**Sal-epiNH$_2$**) was resynthesized following the previously reported procedure,[26] with slight modifications.

Briefly, in the first step, to a stirred solution of salinomycin (**Sal**) (3.00 g, 1.0 equiv) in 50 mL of CH_2Cl_2 in an ice bath were added DMAP (2.38 g, 5.0 equiv), TMSEtOH (2.77 g, 6.0 equiv), and TCFH (1.31 g, 1.2 equiv). The resulting mixture was stirred at RT overnight. The reaction mixture was then concentrated under reduced pressure. Purification on silica gel using the CombiFlash system (0 → 40% EtOAc/*n*-hexane) gave the C1-EtTMS ester of **Sal** as a yellow oil (1.70 g, 50% yield).

Next, to a solution of the C1-EtTMS ester of **Sal** (1.70 g, 1.0 equiv) in 20 mL of anhydrous THF in an ice bath was added TPP (784 mg, 1.5 equiv). After 20 min, DIAD (481 mg, 1.2 equiv) was slowly added to the mixture, followed by DPPA (605 mg, 1.1 equiv). The solution was stirred at RT for 24 h. After this time, TPP (1.57 g, 3.0 equiv) was added to the mixture in one portion, followed by the addition of 0.5 mL of water. The mixture was stirred at RT for next 24 h, and the reaction progress was monitored by TLC. The reaction mixture was then concentrated under reduced pressure. Purification on silica gel using the CombiFlash system (0 → 50% acetone/$CHCl_3$) gave the C1-EtTMS ester of C20-*epi*-aminosalinomycin as a yellow oil (716 mg, 42% yield).

Finally, the C1-masked C20-*epi*-aminosalinomycin (716 mg, 1.0 equiv) was dissolved in 15 mL of anhydrous THF at RT. A 1.0 M solution of TBAF in THF (2.53 mL, 3.0 equiv) was then added dropwise. The solution was left to be stirred at RT for next 24 h. The reaction mixture was then concentrated under reduced pressure. Purification on silica gel using the CombiFlash system (0 → 50% acetone/$CHCl_3$) gave the reaction product as a yellow oil. The product was then dissolved in CH_2Cl_2 and washed with a 0.1 M solution of Na_2CO_3. The separated organic layers were dried over $MgSO_4$ and concentrated under reduced pressure. The residue was then evaporated several times with *n*-pentane to quantitatively give the sodium salt of **Sal-epiNH$_2$** as a white amorphous solid (648 mg). The data for the obtained material were in accordance with the literature.

4.2. General Procedure for the Preparation of Analogs 1−18

To a stirred solution of **Sal-epiNH$_2$** (50 mg, 0.07 mmol, 1.0 equiv) in 5 mL of CH_2Cl_2 was added the corresponding aldehyde (1.0 equiv for singly substituted analogs **1**−**7** and **14**−**18** or 5.0 equiv for the doubly substituted counterparts **8**−**13**). The solution was stirred at RT for 24 h. After that time, a solution of $NaBH_3CN$ (5 mg, 0.08 mmol, 1.2 equiv; in 2 mL of MeOH) was added to the mixture drop by drop. The reaction mixture was stirred further at RT for an additional 30 min. Next, the solvent was evaporated under reduced pressure. Purification of the crude material on silica gel using the CombiFlash system gave the C20-*epi*-amino analogs **1**−**18** as white amorphous solids after evaporation with *n*-pentane. The NMR and HRMS spectra of compounds **1**−**18** are included in the Supporting Information (Figures S1−S54).

4.2.1. Compound 1. Yield: 35 mg, 70%. Isolated as a white amorphous solid, >95% pure by NMR and a single spot by TLC; R_f = 0.57 in 60% acetone/$CHCl_3$. Strain green with PMA; ^{1}H NMR (400 MHz, CD_2Cl_2) δ 6.31 (dd, J = 10.7, 5.6 Hz, 1H), 6.12 (d, J = 10.8 Hz, 1H), 4.29 (q, J = 6.8 Hz, 1H), 4.12 (d, J = 10.4 Hz, 1H), 3.77 (dt, J = 13.8, 6.9 Hz, 1H), 3.64 (dd, J = 10.1, 2.1 Hz, 1H), 3.60 (d, J = 10.2 Hz, 1H), 3.37 (dd, J = 11.9, 2.1 Hz, 1H), 2.86 (d, J = 5.6 Hz, 1H), 2.81−2.73 (m, 2H), 2.72−2.68 (m, 1H), 2.67−2.57 (m, 2H), 2.00−0.50 (m, 60H) ppm; ^{13}C NMR (101 MHz, CD_2Cl_2) δ 218.4, 184.1, 129.9, 122.7, 110.1, 99.7, 89.2, 76.4, 76.3, 75.5, 75.1, 71.8, 70.2, 67.7, 56.1, 55.5, 51.6, 50.9, 42.8, 40.7, 39.5, 37.5, 36.5, 33.4, 33.1, 33.0, 29.8, 28.6, 28.3, 27.4, 24.2, 21.4, 20.6, 17.9, 17.3, 16.5, 16.4, 15.1, 13.5, 12.8, 12.4, 11.0, 7.0, 6.8 ppm; FT-IR (KBr) 3319, 2963, 2935, 2875, 1714, 1568, 1460, 1407 cm^{-1}. HRMS (ESI$^+$) m/z [M + H]$^+$ Calcd for $C_{44}H_{75}NO_{10}Na^+$ 800.5289, found 800.5283; [M − Na + 2H]$^+$ Calcd for $C_{44}H_{76}NO_{10}^+$ 778.5464, found 778.5460.

4.2.2. Compound 2. Yield: 35 mg, 66%. Isolated as a white amorphous solid, >95% pure by NMR and a single spot by TLC; R_f = 0.23 in 66% EtOAc/*n*-hexane. Strain green with PMA; ^{1}H NMR (400 MHz, CD_2Cl_2) δ 6.27 (dd, J = 10.7, 5.6 Hz, 1H), 6.08 (d, J = 10.8 Hz, 1H), 4.28 (q, J = 6.7 Hz, 1H), 4.11 (d, J = 10.2 Hz, 1H), 3.78 (dd, J = 11.1, 4.8 Hz, 1H), 3.64 (dd, J = 16.6, 6.3 Hz, 2H), 3.37 (dd, J = 11.9, 2.1 Hz, 1H), 2.97−2.87 (m, 2H), 2.79−2.68 (m, 2H), 2.68−2.61 (m, 1H), 2.11−2.04 (m, 2H), 2.00−0.50 (m, 61H) ppm; ^{13}C NMR (101 MHz, CD_2Cl_2) δ 218.6, 184.1, 130.3, 122.0, 110.4, 99.6, 89.22, 76.5, 76.4, 75.4, 75.1, 71.8, 70.2, 67.8, 56.1, 53.3, 51.6, 50.9, 47.6, 40.7, 39.5, 37.7, 36.5, 33.3, 33.2, 33.0, 30.0, 28.6, 28.2, 27.5, 24.8, 24.1, 23.2, 21.3, 20.6, 17.9, 17.4, 16.6, 15.1, 13.5, 12.8, 12.4, 11.0, 7.1, 6.8 ppm; FT-IR (KBr) 3289, 2962, 2933, 2874, 1713, 1660, 1568, 1459, 1407 cm^{-1}. HRMS (ESI$^+$) m/z [M + H]$^+$ Calcd for $C_{45}H_{77}NO_{10}Na^+$ 814.5440, found 814.5426; [M − Na + 2H]$^+$ Calcd for $C_{45}H_{78}NO_{10}^+$ 792.5620, found 792.5619.

4.2.3. Compound 3. Yield: 36 mg, 68%. Isolated as a white amorphous solid, >95% pure by NMR and a single spot by TLC; R_f = 0.29 in 66% EtOAc/*n*-hexane. Strain green with PMA; ^{1}H NMR (400 MHz, CD_2Cl_2) δ 6.31 (dd, J = 10.7, 5.6 Hz, 1H), 6.11 (d, J = 10.8 Hz, 1H), 4.29 (q, J = 6.7 Hz, 1H), 4.12 (d, J = 10.4 Hz, 1H), 3.78 (dd, J = 11.1, 4.8 Hz, 1H), 3.64 (dd, J = 9.9, 1.8 Hz, 1H), 3.60 (d, J = 10.2 Hz, 1H), 3.37 (dd, J = 11.9, 2.1 Hz, 1H), 2.84 (d, J = 5.6 Hz, 1H), 2.80−2.69 (m, 3H), 2.68−2.62 (m, 1H), 2.60−2.52 (m, 1H), 2.00−0.50 (m, 64H) ppm; ^{13}C NMR (101 MHz, CD_2Cl_2) δ 218.4, 184.1, 130.0, 122.6, 110.1, 99.7, 89.2, 76.4, 76.3, 75.5, 75.0, 71.8, 70.2, 67.7, 56.1, 55.8, 51.6, 50.9, 48.3, 40.7, 39.4, 37.5, 36.5, 33.5, 33.4, 33.1, 33.0, 29.8, 28.6, 28.3, 27.4, 24.2, 21.4, 20.8, 20.6, 17.8, 17.3, 16.5, 15.1, 14.3, 13.5, 12.8, 12.4, 11.0, 7.0, 6.8 ppm; FT-IR (KBr) 3288, 2960, 2931, 2873, 1713, 1661, 1567, 1459, 1406 cm^{-1}. HRMS (ESI$^+$) m/z [M + H]$^+$ Calcd for $C_{46}H_{79}NO_{10}Na^+$ 828.5596, found 828.5577; [M − Na + 2H]$^+$ Calcd for $C_{46}H_{80}NO_{10}^+$ 806.5777, found 806.5772.

4.2.4. Compound 4. Yield: 40 mg, 74%. Isolated as a white amorphous solid, >95% pure by NMR and a single spot by TLC; R_f = 0.50 in 66% EtOAc/*n*-hexane. Strain green with PMA; ^{1}H NMR (400

https://doi.org/10.1021/acsorginorgau.1c00046
ACS Org. Inorg. Au 2022, 2, 214−221

MHz, CD_2Cl_2) δ 6.35 (dd, J = 10.7, 5.6 Hz, 1H), 6.15 (d, J = 10.8 Hz, 1H), 4.33 (q, J = 6.8 Hz, 1H), 4.16 (d, J = 9.4 Hz, 1H), 3.81 (dd, J = 11.1, 4.9 Hz, 1H), 3.72−3.60 (m, 2H), 3.41 (dd, J = 12.0, 2.1 Hz, 1H), 2.85 (d, J = 5.6 Hz, 1H), 2.82−2.73 (m, 2H), 2.72−2.65 (m, 1H), 2.62 (dd, J = 11.3, 6.7 Hz, 1H), 2.41 (dd, J = 11.3, 6.6 Hz, 1H), 2.15−2.09 (m, 2H), 2.05−0.50 (m, 62H) ppm; ^{13}C NMR (101 MHz, CD_2Cl_2) δ 218.3, 184.1, 130.0, 122.5, 110.2, 99.7, 89.2, 76.4, 76.3, 75.5, 75.0, 71.8, 70.2, 67.7, 56.7, 56.0 (2C), 51.6, 50.8, 40.7, 39.4, 37.6, 36.5, 33.4, 33.2, 33.0, 29.8, 29.7, 28.6, 28.3, 27.4, 24.2, 21.3, 20.8, 20.7, 20.5, 17.8, 17.4, 16.5, 15.1, 13.5, 12.8, 12.4, 11.0, 7.0, 6.8 ppm; FT-IR (KBr) 3289, 2960, 2931, 2874, 1713, 1660, 1568, 1459, 1407 cm^{-1}. HRMS (ESI$^+$) m/z [M + H]$^+$ Calcd for $C_{46}H_{79}NO_{10}Na^+$ 828.5596, found 828.5578; [M − Na + 2H]$^+$ Calcd for $C_{46}H_{80}NO_{10}^+$ 806.5777, found 806.5771.

4.2.5. Compound 5. Yield: 45 mg, 82%. Isolated as a white amorphous solid, >95% pure by NMR and a single spot by TLC; R_f = 0.30 in 66% EtOAc/*n*-hexane. Strain green with PMA; ^{1}H NMR (400 MHz, CD_2Cl_2) δ 6.23 (dd, J = 10.7, 5.6 Hz, 1H), 6.03 (d, J = 10.8 Hz, 1H), 4.21 (q, J = 6.7 Hz, 1H), 4.04 (d, J = 10.4 Hz, 1H), 3.70 (dd, J = 11.1, 4.8 Hz, 1H), 3.62−3.49 (m, 2H), 3.29 (dd, J = 11.9, 2.1 Hz, 1H), 2.76 (d, J = 5.6 Hz, 1H), 2.71−2.60 (m, 3H), 2.60−2.53 (m, 1H), 2.48 (ddd, J = 11.3, 7.5, 6.4 Hz, 1H), 2.02−1.96 (m, 2H), 1.90−0.50 (m, 64H) ppm; ^{13}C NMR (101 MHz, CD_2Cl_2) δ 218.4, 184.1, 130.0, 122.6, 110.1, 99.7, 89.2, 76.5, 76.3, 75.5, 75.1, 71.8, 70.2, 67.7, 56.1, 55.8, 51.6, 50.9, 48.6, 40.7, 39.5, 37.5, 36.5, 33.4, 33.2, 33.0, 31.1, 29.9, 29.8, 28.6, 28.3, 27.5, 24.2, 23.1, 21.4, 20.6, 17.9, 17.4, 16.6, 15.1, 14.4, 13.5, 12.8, 12.4, 11.0, 7.0, 6.8 ppm; FT-IR (KBr) 3292, 2961, 2932, 2873, 1713, 1660, 1567, 1459, 1406 cm^{-1}. HRMS (ESI$^+$) m/z [M + H]$^+$ Calcd for $C_{47}H_{81}NO_{10}Na^+$ 842.5753, found 842.5728; [M − Na + 2H]$^+$ Calcd for $C_{47}H_{82}NO_{10}^+$ 820.5933, found 820.5926.

4.2.6. Compound 6. Yield: 37 mg, 70%. Isolated as a white amorphous solid, >95% pure by NMR and a single spot by TLC; R_f = 0.31 in 66% EtOAc/*n*-hexane. Strain green with PMA; ^{1}H NMR (400 MHz, CD_2Cl_2) δ 6.31 (dd, J = 10.7, 5.6 Hz, 1H), 6.11 (d, J = 10.7 Hz, 1H), 4.29 (q, J = 6.7 Hz, 1H), 4.12 (d, J = 10.3 Hz, 1H), 3.78 (dd, J = 11.0, 4.9 Hz, 1H), 3.64 (dd, J = 10.0, 1.7 Hz, 1H), 3.60 (d, J = 10.1 Hz, 1H), 3.37 (dd, J = 11.9, 1.7 Hz, 1H), 2.84 (d, J = 5.6 Hz, 1H), 2.79−2.69 (m, 3H), 2.68−2.62 (m, 1H), 2.56 (dt, J = 11.3, 6.8 Hz, 1H), 2.08−2.02 (m, 2H), 2.00−0.50 (m, 66H) ppm; ^{13}C NMR (101 MHz, CD_2Cl_2) δ 217.8, 183.5, 129.4, 122.0, 109.5, 99.1, 88.6, 75.9, 75.7, 74.9, 74.5, 71.2, 69.6, 67.1, 55.5, 55.2, 51.0, 50.3, 48.0, 40.1, 38.9, 36.9, 35.9, 32.8, 32.6, 32.4, 31.7, 30.7, 29.2, 28.0, 27.7, 26.9, 26.8, 23.6, 22.6, 20.8, 20.0, 17.3, 16.8, 16.0, 14.5, 13.8, 12.9, 12.3, 11.8, 10.4, 6.5, 6.2 ppm; FT-IR (KBr) 3297, 2958, 2930, 2872, 2858, 1714, 1668, 1565, 1459, 1406 cm^{-1}. HRMS (ESI$^+$) m/z [M + H]$^+$ Calcd for $C_{48}H_{83}NO_{10}Na^+$ 856.5909, found 856.5889; [M − Na + 2H]$^+$ Calcd for $C_{48}H_{84}NO_{10}^+$ 834.6090, found 834.6084.

4.2.7. Compound 7. Yield: 60 mg, 85%. Isolated as a white amorphous solid, >95% pure by NMR and a single spot by TLC; R_f = 0.40 in 66% EtOAc/*n*-hexane. Strain green with PMA; ^{1}H NMR (400 MHz, CD_2Cl_2) δ 6.31 (dd, J = 10.7, 5.6 Hz, 1H), 6.11 (d, J = 10.8 Hz, 1H), 4.28 (dd, J = 13.5, 6.7 Hz, 1H), 4.12 (d, J = 10.4 Hz, 1H), 3.77 (dd, J = 11.1, 4.7 Hz, 1H), 3.64 (dd, J = 10.1, 2.0 Hz, 1H), 3.59 (d, J = 10.2 Hz, 1H), 3.37 (dd, J = 11.9, 2.1 Hz, 1H), 2.83 (d, J = 5.6 Hz, 1H), 2.79−2.73 (m, 1H), 2.74−2.68 (m, 2H), 2.68−2.61 (m, 1H), 2.55 (ddd, J = 11.3, 7.4, 6.3 Hz, 1H), 2.10−2.03 (m, 2H), 2.00−0.50 (m, 78H) ppm; ^{13}C NMR (101 MHz, CD_2Cl_2) δ 218.1, 183.9, 129.7, 122.4, 109.9, 99.5, 89.0, 76.2, 76.0, 75.3, 74.8, 71.6, 70.0, 67.4, 55.8, 55.5, 51.3, 50.6, 48.3, 40.5, 39.2, 37.3, 36.3, 33.2, 32.9, 32.8, 32.3, 31.2, 30.0 (3C), 29.9, 29.7, 29.6, 28.4, 28.1, 27.5, 27.2, 24.0, 23.1, 21.1, 20.3, 17.6, 17.2, 16.3, 14.9, 14.3, 13.3, 12.6, 12.2, 10.8, 6.8, 6.6 ppm, one signal overlapped; FT-IR (KBr) 3288, 2960, 2927, 2854, 1713, 1568, 1459, 1406 cm^{-1}. HRMS (ESI$^+$) m/z [M + H]$^+$ Calcd for $C_{54}H_{95}NO_{10}Na^+$ 940.6848, found 940.6829; [M − Na + 2H]$^+$ Calcd for $C_{54}H_{96}NO_{10}^+$ 918.7029, found 918.7024.

4.2.8. Compound 8. Yield: 41 mg, 76%. Isolated as a white amorphous solid, >95% pure by NMR and a single spot by TLC; R_f = 0.42 in 33% EtOAc/*n*-hexane. Strain green with PMA; ^{1}H NMR (400 MHz, CD_2Cl_2) δ 6.28 (dd, J = 11.0, 1.6 Hz, 1H), 5.98 (dd, J = 11.0, 4.2 Hz, 1H), 4.22 (q, J = 6.7 Hz, 1H), 4.11 (d, J = 10.2 Hz, 1H), 3.79 (dd, J = 11.1, 4.8 Hz, 1H), 3.63 (d, J = 10.1 Hz, 2H), 3.38 (dd, J = 12.0, 2.1 Hz, 2H), 2.75 (td, J = 11.2, 3.3 Hz, 1H), 2.69−2.64 (m, 2H), 2.56−2.43 (m, 3H), 2.31 (dq, J = 13.4, 6.7 Hz, 2H), 2.20−0.50 (m, 61H) ppm; ^{13}C NMR (101 MHz, CD_2Cl_2) δ 218.4, 183.7, 125.6, 123.9, 110.9, 98.0, 87.3, 76.1, 75.8, 75.1, 74.9, 71.2, 69.5, 67.1, 56.4, 55.7, 51.0, 50.1, 44.4, 40.4, 38.6, 36.7, 35.9, 33.0, 32.6, 32.4, 29.8, 28.0, 27.6, 26.9 (2C), 23.6, 21.1, 19.9, 17.3, 16.8, 15.7, 14.6, 13.7 (2C), 12.8, 12.2, 12.0, 10.4, 6.5, 6.2 ppm; FT-IR (KBr) 3300, 2962, 2933, 2874, 1714, 1566, 1458, 1405 cm^{-1}. HRMS (ESI$^+$) m/z [M + H]$^+$ Calcd for $C_{46}H_{79}NO_{10}Na^+$ 828.5596, found 828.5582; [M − Na + 2H]$^+$ Calcd for $C_{46}H_{80}NO_{10}^+$ 806.5777, found 806.5774.

4.2.9. Compound 9. Yield: 45 mg, 79%. Isolated as a white amorphous solid, >95% pure by NMR and a single spot by TLC; R_f = 0.57 in 33% EtOAc/*n*-hexane. Strain green with PMA; ^{1}H NMR (400 MHz, CD_2Cl_2) δ 6.28 (dd, J = 11.0, 1.7 Hz, 1H), 6.00 (dd, J = 11.0, 4.2 Hz, 1H), 4.22 (q, J = 6.8 Hz, 1H), 4.11 (d, J = 10.3 Hz, 1H), 3.79 (dd, J = 11.1, 4.8 Hz, 1H), 3.68−3.59 (m, 2H), 3.37 (dd, J = 12.0, 2.1 Hz, 1H), 3.30 (dd, J = 4.2, 1.8 Hz, 1H), 2.77−2.70 (m, 1H), 2.69−2.63 (m, 2H), 2.52−2.41 (m, 1H), 2.40−2.25 (m, 4H), 2.00−0.50 (m, 65H) ppm; ^{13}C NMR (101 MHz, CD_2Cl_2) δ 219.0, 184.2, 126.3, 124.4, 111.6, 98.7, 87.9, 76.7, 76.4, 75.6, 75.4, 71.8, 70.0, 67.7, 57.9, 56.3, 53.7 (2C), 51.6, 50.8, 41.1, 39.2, 37.3, 36.5, 33.6, 33.3, 33.0, 30.4, 28.6, 28.2, 27.5, 24.1, 22.1 (2C), 21.7, 20.5, 17.9, 17.5, 16.3, 15.2, 13.4, 12.8, 12.6, 12.1 (2C), 11.0, 7.1, 6.7 ppm; FT-IR (KBr) 3297, 2960, 2933, 2873, 1714, 1566, 1459, 1406 cm^{-1}. HRMS (ESI$^+$) m/z [M + H]$^+$ Calcd for $C_{48}H_{83}NO_{10}Na^+$ 856.5909, found 856.5892; [M − Na + 2H]$^+$ Calcd for $C_{48}H_{84}NO_{10}^+$ 834.6090, found 834.6089.

4.2.10. Compound 10. Yield: 30 mg, 55%. Isolated as a white amorphous solid, >95% pure by NMR and a single spot by TLC; R_f = 0.59 in 33% EtOAc/*n*-hexane. Strain green with PMA; ^{1}H NMR (400 MHz, CD_2Cl_2) δ 6.29 (dd, J = 11.0, 1.7 Hz, 1H), 6.01 (dd, J = 11.0, 4.2 Hz, 1H), 4.20 (q, J = 6.7 Hz, 1H), 4.11 (d, J = 10.2 Hz, 1H), 3.79 (dd, J = 11.1, 4.8 Hz, 1H), 3.66−3.60 (m, 2H), 3.37 (dd, J = 12.0, 2.1 Hz, 1H), 3.30 (dd, J = 4.2, 1.7 Hz, 1H), 2.77−2.64 (m, 3H), 2.51−2.35 (m, 3H), 2.34−2.25 (m, 2H),2.00−0.50 (m, 69H) ppm; ^{13}C NMR (101 MHz, CD_2Cl_2) δ 218.9, 184.2, 126.1, 124.4, 111.6, 98.7, 87.9, 76.9, 76.4, 75.6, 75.3, 71.8, 69.9, 67.6, 57.7, 56.2, 51.6, 51.4 (2C), 50.8, 41.1, 39.2, 37.4, 36.5, 33.6, 33.3, 32.9, 31.5 (2C), 30.2, 28.6, 28.2, 27.5, 24.2, 21.7, 21.2 (2C), 20.5, 17.9, 17.5, 16.3, 15.2, 14.5 (2C), 13.4, 12.9, 12.6, 11.0, 7.1, 6.7 ppm; FT-IR (KBr) 3300, 2960, 2933, 2873, 2860, 1712, 1566, 1457, 1406 cm^{-1}. HRMS (ESI$^+$) m/z [M + H]$^+$ Calcd for $C_{50}H_{87}NO_{10}Na^+$ 884.6222, found 884.6212; [M − Na + 2H]$^+$ Calcd for $C_{50}H_{88}NO_{10}^+$ 862.6403, found 862.6410.

4.2.11. Compound 11. Yield: 35 mg, 60%. Isolated as a white amorphous solid, >95% pure by NMR and a single spot by TLC; R_f = 0.62 in 33% EtOAc/*n*-hexane. Strain green with PMA; ^{1}H NMR (400 MHz, CD_2Cl_2) δ 6.29 (dd, J = 11.0, 1.6 Hz, 1H), 6.01 (dd, J = 11.0, 4.2 Hz, 1H), 4.19 (q, J = 6.7 Hz, 1H), 4.11 (d, J = 10.3 Hz, 1H), 3.79 (dd, J = 11.0, 4.7 Hz, 1H), 3.69−3.60 (m, 2H), 3.37 (dd, J = 12.0, 1.9 Hz, 1H), 3.29 (dd, J = 4.1, 1.6 Hz, 1H), 2.70 (tdd, J = 10.3, 9.3, 3.1 Hz, 3H), 2.45 (ddd, J = 22.3, 13.0, 7.1 Hz, 2H), 2.39−2.25 (m, 3H), 2.00−0.50 (m, 73H) ppm; ^{13}C NMR (101 MHz, CD_2Cl_2) δ 218.9, 184.2, 126.1, 124.4, 111.6, 98.7, 87.9, 77.0, 76.4, 75.6, 75.3, 71.8, 69.9, 67.7, 57.8, 56.3, 51.7 (2C), 51.6, 50.8, 41.1, 39.2, 37.4, 36.5, 33.6, 33.3, 32.9, 30.3 (2C), 30.1, 29.0 (2C), 28.6, 28.2, 27.5, 24.2, 23.2 (2C), 21.7, 20.5, 17.9, 17.5, 16.3, 15.2, 14.5 (2C), 13.4, 12.9, 12.6, 11.0, 7.1, 6.7 ppm; FT-IR (KBr) 3297, 2959, 2931, 2872, 2860, 1714, 1567, 1459, 1406 cm^{-1}. HRMS (ESI$^+$) m/z [M + H]$^+$ Calcd for $C_{52}H_{91}NO_{10}Na^+$ 912.6535, found 912.6524; [M − Na + 2H]$^+$ Calcd for $C_{52}H_{92}NO_{10}^+$ 890.6716, found 890.6724.

4.2.12. Compound 12. Yield: 50 mg, 82%. Isolated as a white amorphous solid, >95% pure by NMR and a single spot by TLC; R_f = 0.64 in 33% EtOAc/*n*-hexane. Strain green with PMA; ^{1}H NMR (400 MHz, CD_2Cl_2) δ 6.29 (dd, J = 11.0, 1.6 Hz, 1H), 6.01 (dd, J = 11.0, 4.2 Hz, 1H), 4.20 (q, J = 6.7 Hz, 1H), 4.12 (d, J = 10.3 Hz, 1H), 3.78 (dt, J = 13.2, 6.5 Hz, 1H), 3.68−3.59 (m, 2H), 3.38 (dd, J = 12.0, 1.9 Hz, 1H), 3.29 (dd, J = 4.1, 1.6 Hz, 1H), 2.72 (ddd, J = 11.4, 8.5, 3.4 Hz, 2H), 2.68−2.63 (m, 1H), 2.52−2.43 (m, 1H), 2.43−2.36 (m, 2H), 2.36−2.27 (m, 2H), 2.00−0.50 (m, 77H) ppm; ^{13}C NMR (101 MHz, CD_2Cl_2) δ 218.9, 184.2, 126.1, 124.4, 111.6, 98.7, 87.9, 77.0, 76.4, 75.6, 75.3, 71.8, 69.9, 67.7, 57.8, 56.3, 51.7 (2C), 51.6, 50.8, 41.1, 39.2, 37.4, 36.5, 33.6, 33.3, 33.0, 32.5 (2C), 30.0, 29.3 (2C), 28.6, 28.2, 27.8 (2C),

https://doi.org/10.1021/acsorginorgau.1c00046
ACS Org. Inorg. Au 2022, 2, 214−221

27.5, 24.2, 23.4 (2C), 21.7, 20.5, 17.9, 17.6, 16.3, 15.2, 14.5 (2C), 13.5, 12.9, 12.6, 11.0, 7.1, 6.8 ppm; FT-IR (KBr) 3286, 2960, 2931, 2873, 2859, 1713, 1568, 1459, 1407 cm^{-1}. HRMS (ESI^+) m/z $[M + H]^+$ Calcd for $C_{54}H_{95}NO_{10}Na^+$ 940.6848, found 940.6839; $[M - Na + 2H]^+$ Calcd for $C_{54}H_{96}NO_{10}^+$ 918.7029, found 918.7038.

4.2.13. Compound 13. Yield: 21 mg, 45%. Isolated as a white amorphous solid, >95% pure by NMR and a single spot by TLC; R_f = 0.79 in 33% EtOAc/*n*-hexane. Strain green with PMA; ^1H NMR (400 MHz, CD_2Cl_2) δ 6.28 (dd, J = 11.0, 1.6 Hz, 1H), 6.00 (dd, J = 11.0, 4.2 Hz, 1H), 4.20 (q, J = 6.6 Hz, 1H), 4.11 (d, J = 10.3 Hz, 1H), 3.79 (dd, J = 11.0, 4.6 Hz, 1H), 3.71−3.59 (m, 2H), 3.38 (dd, J = 12.0, 1.9 Hz, 1H), 3.29 (dd, J = 4.1, 1.5 Hz, 1H), 2.75 (dd, J = 11.1, 3.2 Hz, 1H), 2.71−2.64 (m, 2H), 2.47 (dd, J = 12.5, 3.6 Hz, 1H), 2.43−2.38 (m, 1H), 2.36 (d, J = 8.1 Hz, 1H), 2.34−2.25 (m, 2H), 2.00−0.50 (m, 101H) ppm; ^{13}C NMR (101 MHz, CD_2Cl_2) δ 218.9, 184.2, 126.1, 124.4, 111.6, 98.7, 87.9, 76.9, 76.4, 75.6, 75.3, 71.7, 69.9, 67.6, 57.7, 56.3, 51.7 (2C), 51.6, 50.8, 41.1 (2C), 39.2, 37.4, 36.5, 33.6, 33.3, 32.9, 32.5 (2C), 30.6, 30.4 (3C), 30.3, 30.2 (4C), 30.0 (3C), 29.9, 29.3, 28.6, 28.2, 28.1 (2C), 27.5, 24.2, 23.3 (2C), 21.7, 20.5, 17.9, 17.6, 16.3, 15.2, 14.5 (2C), 13.4, 12.9, 12.6, 11.0, 7.1, 6.8 ppm; FT-IR (KBr) 3295, 2958, 2926, 2872, 2854, 1714, 1566, 1459, 1405 cm^{-1}. HRMS (ESI^+) m/z $[M + H]^+$ Calcd for $C_{66}H_{119}NO_{10}Na^+$ 1108.8726, found 1108.8715; $[M - Na + 2H]^+$ Calcd for $C_{66}H_{120}NO_{10}^+$ 1086.8907, found 1086.8920.

4.2.14. Compound 14. Yield: 48 mg, 75%. Isolated as a white amorphous solid, >95% pure by NMR and a single spot by TLC; R_f = 0.65 in 50% EtOAc/*n*-hexane. Strain green with PMA; ^1H NMR (400 MHz, CD_2Cl_2) δ 7.19 (d, J = 4.4 Hz, 4H), 7.12 (dt, J = 5.9, 4.2 Hz, 1H), 6.28 (dd, J = 10.7, 5.6 Hz, 1H), 6.09 (d, J = 10.7 Hz, 1H), 4.18 (q, J = 6.7 Hz, 1H), 4.04 (d, J = 10.4 Hz, 1H), 3.83 (d, J = 12.7 Hz, 1H), 3.74−3.63 (m, 2H), 3.61−3.50 (m, 2H), 3.26 (dd, J = 11.8, 1.8 Hz, 1H), 2.90 (d, J = 5.5 Hz, 1H), 2.73−2.65 (m, 1H), 2.64−2.54 (m, 2H), 2.00−0.50 (m, 57H) ppm; ^{13}C NMR (101 MHz, CD_2Cl_2) δ 218.4, 184.1, 141.5, 129.3, 128.8 (4C), 127.3, 123.1, 110.0, 99.7, 89.3, 76.5, 76.3, 75.5, 75.0, 71.8, 70.2, 67.7, 56.1, 55.1, 52.5, 51.6, 50.9, 40.7, 39.4, 37.6, 36.5, 33.4, 33.1, 33.0, 29.7, 28.6, 28.2, 27.4, 24.2, 21.3, 20.5, 17.8, 17.4, 16.5, 15.1, 13.5, 12.9, 12.4, 11.0, 7.0, 6.8 ppm; FT-IR (KBr) 3317, 2961, 2933, 2874, 1713, 1567, 1495, 1458, 1406 cm^{-1}. HRMS (ESI^+) m/z $[M + H]^+$ Calcd for $C_{49}H_{77}NO_{10}Na^+$ 862.5440, found 862.5432; $[M - Na + 2H]^+$ Calcd for $C_{49}H_{78}NO_{10}^+$ 840.5620, found 840.5628.

4.2.15. Compound 15. Yield: 43 mg, 76%. Isolated as a white amorphous solid, >95% pure by NMR and a single spot by TLC; R_f = 0.60 in 50% EtOAc/*n*-hexane. Strain green with PMA; ^1H NMR (400 MHz, CD_2Cl_2) δ 7.12 (td, J = 7.9, 1.6 Hz, 1H), 6.98 (d, J = 6.3 Hz, 1H), 6.77−6.72 (m, 2H), 6.43 (dd, J = 10.7, 5.5 Hz, 1H), 6.29 (d, J = 10.8 Hz, 1H), 4.29 (q, J = 6.7 Hz, 1H), 4.13 (d, J = 10.5 Hz, 1H), 4.05 (d, J = 13.5 Hz, 1H), 3.97 (d, J = 13.4 Hz, 1H), 3.77 (dd, J = 11.1, 4.8 Hz, 1H), 3.63 (dd, J = 16.2, 6.0 Hz, 2H), 3.38 (dd, J = 11.9, 1.9 Hz, 1H), 3.10 (d, J = 5.4 Hz, 1H), 2.78 (dd, J = 11.0, 2.9 Hz, 1H), 2.73 (dd, J = 10.8, 2.4 Hz 1H), 2.66 (dd, J = 10.2, 7.4 Hz, 1H), 2.00−0.50 (m, 58H) ppm; ^{13}C NMR (101 MHz, CD_2Cl_2) δ 218.4, 184.3, 158.4, 129.4, 129.1, 127.7, 125.1, 123.5, 119.7, 116.7, 108.8, 99.9, 89.8, 76.5, 76.2, 75.8, 75.0, 71.8, 70.2, 67.8, 56.0, 55.1, 51.6, 51.2, 50.8, 40.5, 39.3, 37.8, 36.5, 33.4, 33.1, 32.9, 29.7, 28.6, 28.3, 27.4, 24.3, 21.4, 20.5, 17.8, 17.4, 16.5, 15.1, 13.5, 12.9, 12.4, 10.9, 7.0, 6.7 ppm; FT-IR (KBr) 3433, 3320, 2953, 2932, 2872, 1713, 1563, 1456, 1428, 1405 cm^{-1}. HRMS (ESI^+) m/z $[M + H]^+$ Calcd for $C_{49}H_{77}NO_{10}Na^+$ 878.5389, found 878.5381; $[M - Na + 2H]^+$ Calcd for $C_{49}H_{79}NO_{10}^+$ 856.5569, found 856.5575.

4.2.16. Compound 16. Yield: 51 mg, 89%. Isolated as a white amorphous solid, >95% pure by NMR and a single spot by TLC; R_f = 0.63 in 50% EtOAc/*n*-hexane. Strain green with PMA; ^1H NMR (400 MHz, $CDCl_3$) δ 7.15 (d, J = 7.9 Hz, 2H), 7.08 (d, J = 8.2 Hz, 2H), 6.49 (dd, J = 10.7, 5.6 Hz, 1H), 6.19 (d, J = 10.8 Hz, 1H), 4.39 (dd, J = 13.8, 6.9 Hz, 1H), 4.24 (d, J = 10.3 Hz, 1H), 3.90 (dd, J = 11.0, 4.9 Hz, 1H), 3.85 (d, J = 12.5 Hz, 1H), 3.72 (dd, J = 15.5, 7.2 Hz, 2H), 3.56 (d, J = 10.0 Hz, 1H), 3.34−3.29 (m, 1H), 3.03 (d, J = 5.7 Hz, 1H), 2.87 (td, J = 11.0, 3.3 Hz, 1H), 2.68 (dd, J = 11.0, 2.6 Hz, 1H), 2.64−2.59 (m, 1H), 2.31 (s, 3H), 2.20−0.50 (m, 57H) ppm; ^{13}C NMR (101 MHz, $CDCl_3$) δ 216.8, 184.1, 137.7, 136.3, 129.0 (2C), 128.2 (2C), 122.6, 109.3, 99.1, 88.7, 75.7, 75.6, 74.8, 74.5, 71.5, 69.8, 67.1, 55.2, 54.6, 51.6, 51.2, 50.4, 40.1, 38.9, 37.2, 36.0, 32.9, 32.5, 32.4, 29.7, 29.0, 27.9 (2C), 26.9, 23.9, 21.1, 20.8, 19.9, 17.5, 17.0, 16.0, 14.6, 13.2, 12.5, 11.8, 10.6, 6.7, 6.5 ppm; FT-IR (KBr) 3295, 2961, 2931, 2874, 1713, 1567, 1458, 1406 cm^{-1}. HRMS (ESI^+) m/z $[M + H]^+$ Calcd for $C_{50}H_{79}NO_{11}Na^+$ 876.5596, found 876.5593; $[M - Na + 2H]^+$ Calcd for $C_{50}H_{80}NO_{11}^+$ 854.5777, found 854.5777.

4.2.17. Compound 17. Yield: 70 mg, 88%. Isolated as a white amorphous solid, >95% pure by NMR and a single spot by TLC; R_f = 0.67 in 50% EtOAc/*n*-hexane. Strain green with PMA; ^1H NMR (400 MHz, $CDCl_3$) δ 7.22 (dd, J = 8.5, 5.6 Hz, 2H), 6.95 (dd, J = 12.0, 5.3 Hz, 2H), 6.48 (dd, J = 10.7, 5.6 Hz, 1H), 6.20 (d, J = 10.8 Hz, 1H), 4.37 (q, J = 6.6 Hz, 1H), 4.23 (d, J = 10.3 Hz, 1H), 3.89 (dd, J = 11.1, 4.9 Hz, 1H), 3.85 (d, J = 11.9 Hz, 1H), 3.74−3.68 (m, 2H), 3.56 (d, J = 10.1 Hz, 1H), 3.30 (dd, J = 11.9, 1.9 Hz, 1H), 3.00 (d, J = 5.6 Hz, 1H), 2.87 (td, J = 10.9, 3.1 Hz, 1H), 2.67 (dt, J = 7.1, 3.6 Hz, 1H), 2.62 (dd, J = 10.2, 7.4 Hz, 1H), 2.20−0.50 (m, 57H) ppm; ^{13}C NMR (101 MHz, $CDCl_3$) δ 216.8, 184.1, 161.9 (d, J_{C-F} = 191.9 Hz, 1C), 136.4, 129.9 (d, J_{C-F} = 6.2 Hz, 1C), 128.8, 122.8, 115.1 (d, J_{C-F} = 20.2 Hz, 1C), 109.3, 99.1, 88.8, 75.7, 75.7, 74.9, 74.5, 71.6, 69.8, 67.2, 55.3, 54.3, 51.3, 51.0, 50.4, 40.1, 38.9, 37.3, 36.0, 34.1, 32.9, 32.5, 32.4, 29.0, 27.9, 26.9, 24.0, 22.3, 20.9, 20.0, 17.5, 17.0, 16.0, 14.6, 14.1, 13.2, 12.5, 11.8, 10.6, 6.7, 6.5 ppm; FT-IR (KBr) 3321, 2962, 2932, 2874, 1713, 1567, 1510, 1459, 1406 cm^{-1}. HRMS (ESI^+) m/z $[M + H]^+$ Calcd for $C_{49}H_{76}FNO_{10}Na^+$ 880.5345, found 880.5337; $[M - Na + 2H]^+$ Calcd for $C_{49}H_{77}FNO_{10}^+$ 858.5526, found 858.5532.

4.2.18. Compound 18. Yield: 34 mg, 58%. Isolated as a white amorphous solid, >95% pure by NMR and a single spot by TLC; R_f = 0.58 in 50% EtOAc/*n*-hexane. Strain green with PMA; ^1H NMR (400 MHz, $CDCl_3$) δ 7.18 (d, J = 8.8 Hz, 2H), 7.13 (d, J = 8.5 Hz, 2H), 6.42 (dd, J = 10.7, 5.6 Hz, 1H), 6.14 (d, J = 10.8 Hz, 1H), 4.30 (q, J = 6.7 Hz, 1H), 4.17 (d, J = 10.2 Hz, 1H), 3.83 (dd, J = 10.6, 4.2 Hz, 1H), 3.78 (d, J = 12.9 Hz, 1H), 3.68−3.61 (m, 2H), 3.49 (d, J = 10.1 Hz, 1H), 3.23 (d, J = 11.6 Hz, 1H), 2.93 (d, J = 5.6 Hz, 1H), 2.80 (td, J = 10.9, 3.1 Hz, 1H), 2.61 (dd, J = 11.0, 2.4 Hz, 1H), 2.55 (dd, J = 10.2, 7.4 Hz, 1H), 2.20−0.50 (m, 57H) ppm; ^{13}C NMR (101 MHz, $CDCl_3$) δ 216.7, 184.2, 139.1, 132.5, 129.7 (2C), 128.7, 128.4 (2C), 122.8, 109.2, 99.0, 88.7, 75.7, 75.6, 74.9, 74.5, 71.5, 69.8, 67.1, 55.2, 54.3, 51.2, 51.0, 50.4, 40.1, 38.8, 37.3, 35.9, 32.9, 32.5, 32.4, 29.7, 28.9, 27.9 (2C), 23.9, 20.8, 19.9, 17.4, 17.0, 16.0, 14.6, 13.2, 12.5, 11.8, 10.6, 6.7, 6.5 ppm; FT-IR (KBr) 3322, 2962, 2932, 2874, 1713, 1663, 1567, 1492, 1459, 1407 cm^{-1}. HRMS (ESI^+) m/z $[M + H]^+$ Calcd for $C_{49}H_{76}ClNO_{10}Na^+$ 896.5050, found 896.5043; $[M - Na + 2H]^+$ Calcd for $C_{49}H_{77}ClNO_{10}^+$ 874.5231, found 874.5238.

4.3. Cell Culture

HMLER cells naturally repressing E-cadherin, obtained from human mammary epithelial cells infected with a retrovirus carrying hTERT, SV40, and the oncogenic allele *H-rasV12*, were cultured in DMEM/F12 (Gibco, 31331−028) supplemented with 10% FBS, 10 μg/mL insulin (Sigma-Aldrich, I0516), 0.5 μg/mL hydrocortisone (Sigma-Aldrich, H0888), and 0.5 μg/mL puromycin (Life Technologies, A11138-02); cells were a generous gift from Alain Puisieux (INSERM). All cells were incubated at 37 °C with 5% CO_2. HMLER $CD44^{low/high}$ cells stained with CD24-APC and CD44-PE antibodies were sorted by FACS using an Aria IIu (BD Biosciences) to obtain isolated $CD24^{low}/CD44^{high}$ and $CD24^{high}/CD44^{low}$ cell populations. HMLER $CD24^{low}/CD44^{high}$ cells were supplemented with 10 ng/mL human epidermal growth factor (EGF, Miltenyi Biotec, 130-093-750, 100 ng/mL), while HMLER $CD24^{high}/CD44^{low}$ cells were grown without EGF. MCF10A cells (ATCC, CRL-10317) were cultured in DMEM/F12 supplemented with 10% horse serum (Invitrogen, 16050-122), 10 μg/mL insulin, 10 ng/mL EGF, 0.5 μg/mL hydrocortisone, 100 ng/mL cholera toxin (Sigma-Aldrich, C8052), and 1 × PenStrep (Invitrogen, 15070-063).

4.4. Cell Viability Assay (IC_{50})

The cell viability assay was carried out by plating 1000 cells per well in 96-well plates. The cells were treated for 72 h in a range between 12 nM and 50 μM or 0.3 nM and 4 μM using serial dilutions following the manufacturer's protocol. Very briefly, the CellTiter-Blue reagent (G8081, Promega) was added to the wells after 72 h of treatment, and cells were incubated for 3 h before fluorescence intensities (λ_{ex} =

https://doi.org/10.1021/acsorginorgau.1c00046
ACS Org. Inorg. Au 2022, 2, 214−221

560/20 nm; λ_{em} = 590/10 nm) were recorded using a PerkinElmer Wallac 1420 Victor2 microplate reader.

The IC_{50} cell viability curves were plotted using the Prism 8 software for the synthesized compounds against HMLER $CD24^{low}/CD44^{high}$ and the isogenic cell line HMLER $CD24^{high}/CD44^{low}$; MCF10A cells are included in the Supporting Information (Figures S55–S56).

■ ASSOCIATED CONTENT

Supporting Information

The Supporting Information is available free of charge at https://pubs.acs.org/doi/10.1021/acsorginorgau.1c00046.

Detailed descriptions of general procedures, equipment, and measurement parameters; ^{1}H NMR, ^{13}C NMR, and HRMS spectra of new C20-*epi*-amino analogs of salinomycin (**1**–**18**); and IC_{50} cell viability curves (PDF)

■ AUTHOR INFORMATION

Corresponding Authors

Michał Antoszczak − *Department of Chemical Biology Institut Curie, CNRS UMR 3666, INSERM U1143, PSL Université, 75005 Paris, France; Department of Medical Chemistry, Faculty of Chemistry, Adam Mickiewicz University, 61−614 Poznań, Poland;* orcid.org/0000-0003-0877-1726; Phone: +48 61 829 1754; Email: michant@amu.edu.pl

Raphaël Rodriguez − *Department of Chemical Biology Institut Curie, CNRS UMR 3666, INSERM U1143, PSL Université, 75005 Paris, France;* orcid.org/0000-0001-7668-446X; Phone: +33 648 482 191; Email: raphael.rodriguez@curie.fr

Authors

Dominika Czerwonka − *Department of Chemical Biology Institut Curie, CNRS UMR 3666, INSERM U1143, PSL Université, 75005 Paris, France; Department of Medical Chemistry, Faculty of Chemistry, Adam Mickiewicz University, 61−614 Poznań, Poland*

Sebastian Müller − *Department of Chemical Biology Institut Curie, CNRS UMR 3666, INSERM U1143, PSL Université, 75005 Paris, France*

Tatiana Cañeque − *Department of Chemical Biology Institut Curie, CNRS UMR 3666, INSERM U1143, PSL Université, 75005 Paris, France;* orcid.org/0000-0002-1110-0643

Ludovic Colombeau − *Department of Chemical Biology Institut Curie, CNRS UMR 3666, INSERM U1143, PSL Université, 75005 Paris, France*

Adam Huczyński − *Department of Medical Chemistry, Faculty of Chemistry, Adam Mickiewicz University, 61−614 Poznań, Poland*

Complete contact information is available at: https://pubs.acs.org/10.1021/acsorginorgau.1c00046

Author Contributions

R.R. and A.H. directed the research. D.C. designed and synthesized the derivatives. T.C. did the stability tests. D.C., M.A., and S.M. evaluated the compounds *in vitro*. M.A., D.C., and R.R. wrote the article with contributions from S.M., T.C., L.C., and A.H.

Funding

This research was funded by the European Research Council under the European Union's Horizon 2020 research and innovation program Grant 647973 (R.R.), the Foundation Charles Defforey-Institut de France (R.R.), Ligue Contre le Cancer (R.R., Equipe Labelisée), and Region IdF for NMR infrastructure (R.R.).

Notes

The authors declare no competing financial interest.

■ ACKNOWLEDGMENTS

D.C. wishes to acknowledge the Polish Science Center (NCN) for the doctoral scholarship ETIUDA (2020/36/T/ST4/00041) and scholarship no. POWR.03.02.00e00-I026/16, cofinanced by the European Union through the European Social Fund under the Operational Program Knowledge Education Development. M.A. thanks the NCN and the Polish National Agency for Academic Exchange (NAWA) for scholarships under the UWERTURA (2019/32/U/ST4/00092) and the BEKKER programs (PPN/BEK/2019/1/00034), respectively, and the Polish Ministry of Science and Higher Education (MNiSW) for the scholarship for outstanding young scientists in the years 2020−2023 (STYP/15/1665/E-336/2020).

■ ABBREVIATIONS

aq., aqueous
ATP, adenosine triphosphate
CSCs, cancer stem cells
DIAD, diisopropyl azodicarboxylate
DMAP, 4-dimethylaminopyridine
DPPA, diphenylphosphoryl azide
equiv, equivalent(s)
ER, endoplasmic reticulum
ESI, electrospray ionization
EtOAc, ethyl acetate
FT-IR, Fourier-transform infrared spectroscopy
HRMS, high-resolution mass spectroscopy
MeOH, methanol
MoA, mechanism of action
NMR, nuclear magnetic resonance
PMA, phosphomolybdic acid hydrate
ROS, reactive oxygen species
RT, room temperature
Sal, salinomycin
Sal-epiNH$_2$, C20-*epi*-aminosalinomycin
SAR, structure−activity relationship
SI, selectivity index
TBAF, tetrabutylammonium fluoride
TCFH, chloro-*N*,*N*,*N*′,*N*′-tetramethylformamidinium hexafluorophosphate
THF, tetrahydrofuran
TLC, thin-layer chromatography
TMSEtOH, 2-(trimethylsilyl)ethanol
TPP, triphenylphosphine.

■ REFERENCES

(1) World Health Organization. WHO Report on Cancer, 2020. https://www.who.int/publications/i/item/who-report-on-cancer-setting-priorities-investing-wisely-and-providing-care-for-all (accessed 2021-10-07).

(2) Clevers, H. The cancer stem cell: Premises, promises and challenges. *Nat. Med.* **2011**, *17*, 313−319.

(3) Batlle, E.; Clevers, H. Cancer stem cells revisited. *Nat. Med.* **2017**, *23*, 1124−1134.

(4) Reya, T.; Morrison, S. J.; Clarke, M. F.; Weissman, I. L. Stem cells, cancer, and cancer stem cells. *Nature* **2001**, *414*, 105−111.

(5) Kaiser, J. The cancer stem cell gamble. *Science* **2015**, *347*, 226−229.
(6) Gupta, P. B.; Onder, T. T.; Jiang, G.; Tao, K.; Kuperwasser, C.; Weinberg, R. A.; Lander, E. S. Identification of selective inhibitors of cancer stem cells by high-throughput screening. *Cell* **2009**, *138*, 645−659.
(7) Antoszczak, M. A medicinal chemistry perspective on salinomycin as a potent anticancer and anti-CSCs agent. *Eur. J. Med. Chem.* **2019**, *164*, 366−377.
(8) Versini, A.; Saier, L.; Sindikubwabo, F.; Müller, S.; Cañeque, T.; Rodriguez, R. Chemical biology of salinomycin. *Tetrahedron* **2018**, *74*, 5585−5614.
(9) Jangamreddy, J. R.; Ghavami, S.; Grabarek, J.; Kratz, G.; Wiechec, E.; Fredriksson, B. A.; Rao Pariti, R. K.; Cieślar-Pobuda, A.; Panigrahi, S.; Łos, M. J. Salinomycin induces activation of autophagy, mitophagy and affects mitochondrial polarity: Differences between primary and cancer cells. *Biochim. Biophys. Acta Mol. Cell Res.* **2013**, *1833*, 2057−2069.
(10) Boehmerle, W.; Endres, M. Salinomycin induces calpain and cytochrome c-mediated neuronal cell death. *Cell Death Dis.* **2011**, *2*, e168.
(11) Kim, S. H.; Choi, Y. J.; Kim, K. Y.; Yu, S. N.; Seo, Y. K.; Chun, S. S.; Noh, K. T.; Suh, J. T.; Ahn, S. C. Salinomycin simultaneously induces apoptosis and autophagy through generation of reactive oxygen species in osteosarcoma U2OS cells. *Biochem. Biophys. Res. Commun.* **2016**, *473*, 607−613.
(12) Huang, X.; Borgström, B.; Stegmayr, J.; Abassi, Y.; Kruszyk, M.; Leffler, H.; Persson, L.; Albinsson, S.; Massoumi, R.; Scheblykin, I. G.; Hegardt, C.; Oredsson, S.; Strand, D. The molecular basis for inhibition of stemlike cancer cells by salinomycin. *ACS Cent. Sci.* **2018**, *4*, 760−767.
(13) Antoszczak, M. A comprehensive review of salinomycin derivatives as potent anticancer and anti-CSCs agents. *Eur. J. Med. Chem.* **2019**, *166*, 48−64.
(14) Li, B.; Wu, J.; Zhang, W.; Li, Z.; Chen, G.; Zhou, Q.; Wu, S. Synthesis and biological activity of salinomycin-hydroxamic acid conjugates. *Bioorg. Med. Chem. Lett.* **2017**, *27*, 1624−1626.
(15) Borgström, B.; Huang, X.; Chygorin, E.; Oredsson, S.; Strand, D. Salinomycin hydroxamic acids: Synthesis, structure, and biological activity of polyether ionophore hybrids. *ACS Med. Chem. Lett.* **2016**, *7*, 635−640.
(16) Kuran, D.; Flis, S.; Antoszczak, M.; Piskorek, M.; Huczyński, A. Ester derivatives of salinomycin efficiently eliminate breast cancer cells via ER-stress-induced apoptosis. *Eur. J. Pharmacol.* **2021**, *893*, 173824.
(17) Czerwonka, D.; Urbaniak, A.; Sobczak, S.; Piña-Oviedo, S.; Chambers, T. C.; Antoszczak, M.; Huczyński, A. Synthesis and anticancer activity of tertiary amides of salinomycin and their C20-oxo analogues. *ChemMedChem.* **2020**, *15*, 236−246.
(18) Antoszczak, M.; Popiel, K.; Stefańska, J.; Wietrzyk, J.; Maj, E.; Janczak, J.; Michalska, G.; Brzezinski, B.; Huczyński, A. Synthesis, cytotoxicity and antibacterial activity of new esters of polyether antibiotic − salinomycin. *Eur. J. Med. Chem.* **2014**, *76*, 435−444.
(19) Huczyński, A.; Antoszczak, M.; Kleczewska, N.; Lewandowska, M.; Maj, E.; Stefańska, J.; Wietrzyk, J.; Janczak, J.; Celewicz, L. Synthesis and biological activity of salinomycin conjugates with floxuridine. *Eur. J. Med. Chem.* **2015**, *93*, 33−41.
(20) Versini, A.; Colombeau, L.; Hienzsch, A.; Gaillet, C.; Retailleau, P.; Debieu, S.; Müller, S.; Cañeque, T.; Rodriguez, R. Salinomycin derivatives kill breast cancer stem cells by lysosomal iron targeting. *Chem. Eur. J.* **2020**, *26*, 7416−7424.
(21) Mai, T. T.; Hamaï, A.; Hienzsch, A.; Cañeque, T.; Müller, S.; Wicinski, J.; Cabaud, O.; Leroy, C.; David, A.; Acevedo, V.; Ryo, A.; Ginestier, C.; Birnbaum, D.; Charafe-Jauffret, E.; Codogno, P.; Mehrpour, M.; Rodriguez, R. Salinomycin kills cancer stem cells by sequestering iron in lysosomes. *Nat. Chem.* **2017**, *9*, 1025−1033.
(22) Borgström, B.; Huang, X.; Hegardt, C.; Oredsson, S.; Strand, D. Structure-activity relationships in salinomycin: Cytotoxicity and phenotype selectivity of semi-synthetic derivatives. *Chem. Eur. J.* **2017**, *23*, 2077−2083.
(23) Borgström, B.; Huang, X.; Pošta, M.; Hegardt, C.; Oredsson, S.; Strand, D. Synthetic modification of salinomycin: Selective *O*-acylation and biological evaluation. *Chem. Commun.* **2013**, *49*, 9944−9946.
(24) Huang, M.; Deng, Z.; Tian, J.; Liu, T. Synthesis and biological evaluation of salinomycin triazole analogues as anticancer agents. *Eur. J. Med. Chem.* **2017**, *127*, 900−908.
(25) Müller, S.; Sindikubwabo, F.; Cañeque, T.; Lafon, A.; Versini, A.; Lombard, B.; Loew, D.; Wu, T. D.; Ginestier, C.; Charafe-Jauffret, E.; Durand, A.; Vallot, C.; Baulande, S.; Servant, N.; Rodriguez, R. CD44 regulates epigenetic plasticity by mediating iron endocytosis. *Nat. Chem.* **2020**, *12*, 929−938.
(26) Li, Y.; Shi, Q.; Shao, J.; Yuan, Y.; Yang, Z.; Chen, S.; Zhou, X.; Wen, S.; Jiang, Z. X. Synthesis and biological evaluation of 20-*epi*-amino-20-deoxysalinomycin derivatives. *Eur. J. Med. Chem.* **2018**, *148*, 279−290.
(27) Shi, Q.; Li, Y.; Bo, S.; Li, X.; Zhao, P.; Liu, Q.; Yang, Z.; Cong, H.; Deng, H.; Chen, M.; Chen, S.; Zhou, X.; Ding, H.; Jiang, Z. X. Discovery of a ^{19}F MRI sensitive salinomycin derivative with high cytotoxicity towards cancer cells. *Chem. Commun.* **2016**, *52*, 5136−5139.
(28) Zhang, W.; Wu, J.; Li, B.; Xia, J.; Wu, H.; Wang, L.; Hao, J.; Zhou, Q.; Wu, S. Synthesis and biological activity evaluation of 20-*epi*-salinomycin and its 20-*O*-acyl derivatives. *RSC Adv.* **2016**, *6*, 41885−41890.
(29) Czerwonka, D.; Mielczarek-Puta, M.; Antoszczak, M.; Cioch, A.; Struga, M.; Huczyński, A. Evaluation of the anticancer activity of singly and doubly modified analogues of C20-*epi*-salinomycin. *Eur. J. Pharmacol.* **2021**, *908*, 174347.
(30) Morel, A. P.; Lièvre, M.; Thomas, C.; Hinkal, G.; Ansieau, S.; Puisieux, A. Generation of breast cancer stem cells through epithelial-mesenchymal transition. *PLoS One* **2008**, *3*, e2888.
(31) Elenbaas, B.; Spirio, L.; Koerner, F.; Fleming, M. D.; Zimonjic, D. B.; Donaher, J. L.; Popescu, N. C.; Hahn, W. C.; Weinberg, R. A. Human breast cancer cells generated by oncogenic transformation of primary mammary epithelial cells. *Genes Dev.* **2001**, *15*, 50−65.

https://doi.org/10.1021/acsorginorgau.1c00046
ACS Org. Inorg. Au 2022, 2, 214−221